Aalborg Universitet

Detecting creeping thistle in sugar beet fields using vegetation indices

Kazmi, Wajahat; Garcia-Ruiz, Francisco Jose; Nielsen, Jon; Rasmussen, Jesper; Andersen, Hans Jørgen

Detecting creeping thistle in sugar beet fields using vegetation indices

Wajahat Kazmi [a,*], Francisco Jose Garcia-Ruiz [b,1], Jon Nielsen [b,1], Jesper Rasmussen [b,1], Hans Jørgen Andersen [a,2]

[a] Department of Architecture, Design and Media Technology, Aalborg University, Rendsburggade 14, Room: 5 353, 9000 Aalborg, Denmark
[b] Department of Plant and Environmental Sciences, Højbakkegård Allé 9, University of Copenhagen, 2630 Taastrup, Denmark

ABSTRACT

In this article, we address the problem of thistle detection in sugar beet fields under natural, outdoor conditions. In our experiments, we used a commercial color camera and extracted vegetation indices from the images. A total of 474 field images of sugar beet and thistles were collected and divided into six different groups based on illumination, scale and age. The feature set was made up of 14 indices. Mahalanobis Distance (MD) and Linear Discriminant Analysis (LDA) were used to classify the species. Among the features, excess green (ExG), green minus blue (GB) and color index for vegetation extraction (CIVE) offered the highest average accuracy, above 90%. The feature set was reduced to four important indices following a PCA analysis, but the classification accuracy was similar to that obtained by only combining ExG and GB which was around 95%, still better than an individual index. Stepwise linear regression selected nine out of 14 features and offered the highest accuracy of 97%. The results of LDA and MD were fairly close, making them both equally preferable. Finally, the results were validated by annotating images containing both sugar beet and thistles using the trained classifiers. The validation experiments showed that sunlight followed by the size of the plant, which is related to its growth stage, are the two most important factors affecting the classification. In this study, the best results were achieved for images of young sugar beet (in the seventh week) under a shade.

© 2015 Elsevier B.V. All rights reserved.

1. Introduction

Weeds cause crop yield losses with a global average of 34% and which in certain cases, may exceed 70% (Monaco et al., 1981). They compete with crops for nutrients, water and light and therefore, their removal at an early stage is important for a higher crop production.

The most common tool for weed removal is blanket spraying of herbicides which raises environmental concerns. In order to reduce the amount of herbicides, knowledge of when and where to apply them is necessary which is provided by Integrated Weed Management (IWM) and Site Specific Weed Management (SSWM). IWM strives to reduce a weed population to an acceptable level while limiting the impact on the quality of soil, water and other natural resources below a threshold. It uses a combination of biological, mechanical and chemical tools to suppress the weed population at the most effective stages of its life cycle. IWM is complemented by SSWM which describes the techniques for controlling weeds according to their spatial variability in the field (Christensen et al., 2009; Lopez-Granadoz, 2011).

The concept of SSWM narrows the treatment to weed patches (Christensen and Heisel, 2003) or even down to plant scale (Ehsani et al., 2004). This requires sensing and perception technologies and therefore, machine vision is proving vital in agricultural automation.

Canadian or Creeping Thistle (*Cirsium Arvensis* (L.) Scop.) is an invasive perennial weed species that causes major yield loss to Sugar Beet (*Beta vulgaris*). Sugar beet is among the world's important crops, and in 2011 its estimated global production was around 278 million tonnes (FAOSTAT, 2011). Sugar beet industry in Denmark generated more than 137 million USD in 2011 and is becoming the seventh most valuable commodity of the country in terms of revenues (FAOSTAT, 2011). Creeping Thistle (thistle) is becoming increasingly frequent (Andreasen and Stryhn, 2012) and 5–6 plants/m^2 can halve the crop yield (Miller et al., 1994). Tyr and Veres (2012) graded thistles to be one of the two most dangerous perennial weeds for sugar beet stands in Slovak republic.

In order to apply SSWM for thistles, Danish projects such as ASE-TA (Kazmi et al., 2011) has investigated the utility of unmanned

* Corresponding author. Tel: +45 9940 8834.
E-mail addresses: wajahat.kazmi@outlook.com (W. Kazmi), fgr@agromapping.com (F.J. Garcia-Ruiz), jon@plen.ku.dk (J. Nielsen), jer@plen.ku.dk (J. Rasmussen), hja@create.aau.dk (H. Jørgen Andersen).
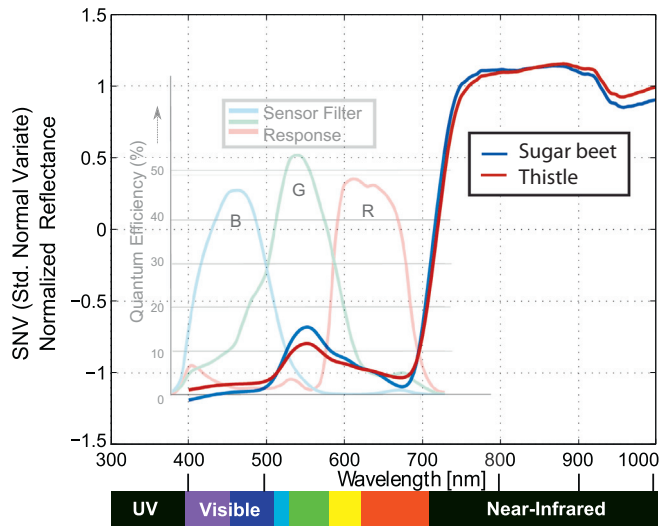[1] Tel: +45 3533 3572.
[2] Tel.: +45 9940 8834.

Fig. 1. Foreground: Spectral signature of Sugar beet and Creeping thistle recorded by Spectra Vista's GER 1500 spectroradiometer. It can be noted that the species have noticeable difference in violet, blue, green and red bands, while the discrimination in Near-Infrared band is also comparable. Background: Filter response of the Bumblebee XB3 camera (Quantum Efficiency curve of the ICX445 sensor) provided by Point Grey Research. Peak values: B(470 nm) = 46%, G(525 nm) = 53%, R(640 nm) = 48%, measured according to EMVA 1288 standard (Point Grey, 2013). (For interpretation of the references to color in this figure legend, the reader is referred to the web version of this article.)

aerial and ground vehicles equipped with advanced imaging sensors. Multi-spectral aerial imaging for the detection of weed patches was investigated as the plant canopies of both sugar beet and thistle show a separation in the spectral response (Fig. 1).

However, to coordinate the aerial detection with subsequent spot treatment, a ground vehicle equipped with a close range imaging system may also be necessary. This is particularly useful for low density patches or single weed plants which are difficult to identify from aerial or satellite platforms (Backes and Jacobi, 2006).

The reduced soil impact, carbon footprint and required human resource for the unmanned ground vehicles (UGV) are making them increasingly famous as a future weed removal technology (another example is European project RHEA (2011)). UGVs can even deploy short range intense lasers to destroy unwanted plants and therefore can completely avoid the use of chemicals (Mathiassen et al., 2006). But for any such scheme to be successful, a sensing system capable of efficiently detecting weeds must be available.

State-of-the-art smart imaging sensors can be highly expensive. This may be affordable with aerial platforms, since fewer aerial vehicles can serve a large field area. But in order to apply timely treatment, several UGVs may be required as the ground vehicles have restricted mobility given the structure and the spread of the plantation inside the fields. Imaging sensors for UGVs must therefore be kept economical and weed detection real-time for a field deployable system.

1.1. Background

For machine vision based weed detection, color vegetation analysis is perhaps the most efficient way. Raw RGB channels and extracted vegetation indices have been widely used, primarily, for vegetation detection against background (Meyer and Neto, 2008; Golzarian et al., 2012).

Extensive work has been done in exploiting vegetation indices for crop/weed classification. Tosaka et al. (1998) used color information to separate vegetation from background and then thinned

out the vegetation to identify sugar beet plants with 55–78% accuracy. El-Faki et al. (2000b) used several color indices to classify three weed species competing each wheat and soyabean. They collected data both outdoor under sunlight and indoor under artificial lighting and achieved an accuracy of 54.9% for soyabean and 62.2% for wheat. Jafari et al. (2006) used stepwise discriminant analysis on the R, G and B color channels for sugar beet and seven types of weeds. They processed the sunlit and shadow datasets separately. The individual weed Correct Classification Rates (CCR) ranged from 79% to 89% producing overall accuracy of 88%. Nieuwenhuizen et al. (2007) used ExG and RB (Red–Blue) index to detect volunteer potato plants among sugar beet, obtaining 49% and 97% accuracy for data from two different fields.

Color indices can be scaled down to pixel classification, but the limiting factor is the separation among the subject plant species in the reflected wavelengths. When the separation is not enough, shape features are used after background subtraction (Pérez et al., 2000), or a combination of color and shape features such as Golzarian and Frick (2011) combined color indices with Waddle Disk Ratio (WDR) which is a measure of roundness of the leaf. Their system was able to classify green house grown wheat from ryegrass and brome grass with an accuracy of 88% and 85% respectively. Åstrand and Baerveldt (2002) used average and standard deviation of the three color channels combined with shape features such as elongation, compactness and perimeter, etc. to detect weeds in sugar beet fields using neural network classifiers.

Approaches for sugar beet so far adopted in literature either do not address thistles (Jafari et al., 2006) or else include them among other weed species and use shape features (Åstrand and Baerveldt, 2002; Sogaard, 2005). Other approaches employ multi-spectral imaging extending from visible to Infrared wavelengths (Feyaerts et al., 1999; Backes and Jacobi, 2006; Vrindts et al., 2002).

1.2. Objective

As can be observed in Fig. 1, there is a noticeable separation between thistle and sugar beet in the blue, green and red spectra. Therefore, the objective in this article is to present a system that can accurately and efficiently detect thistles in sugar beet fields down to plant scale using only vegetation indices thus avoiding shape features which require occlusion detection or segmentation of plant organs (stems or leaves).

2. Materials and methods

Color (RGB) images were acquired using Point Grey's Bumblebee XB3 (Fig. 2(b)). The camera uses three Sony ICX445 1/3″ progressive scan CCD's. One of the three cams were used at the image resolutions and corresponding GSDs (Ground Sample Dis-
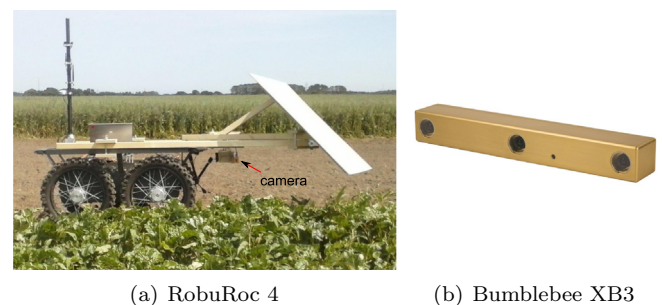

(a) RobuRoc 4 (b) Bumblebee XB3

Fig. 2. Equipment: The unmanned ground vehicle (UGV) and the color camera used in the experiments. (For interpretation of the references to color in this figure legend, the reader is referred to the web version of this article.)
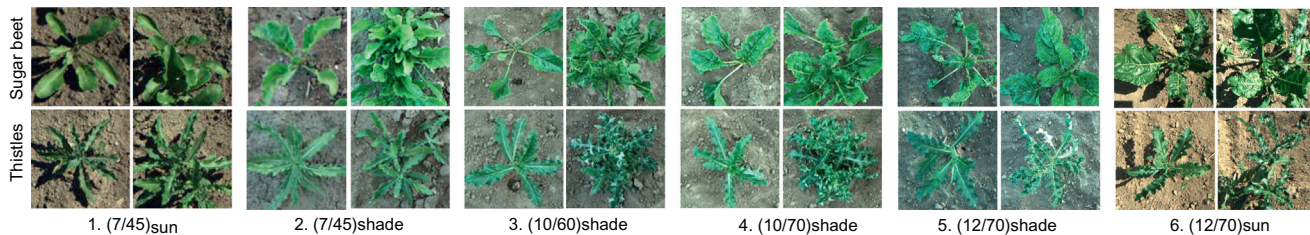
Fig. 3. Some of the sample images of sugar beet and weed (thistle) plants from field data. These images show infield complexities and intra class variations due to wind, light, growth stage and overlapping plant canopies.

tance) given in Table 2. The images were rectified for lens distortion using company calibration. Quantum efficiencies of the Red, Green and Blue filters used in the sensor are shown in the background image of Fig. 1. White balance was activated and factory defaults for channel gains were used as they were found suitable (i.e. Red = 550, Blue = 810 through PGR FlyCapture v1.8 utility). The camera was mounted on a ground vehicle, the robuROC-4 (Fig. 2(a)) (Kazmi et al., 2011), which was operated in a remote control mode. Orientation of camera was vertically downwards. As shown in the figure, an adjustable wooden shade was used to block sunlight from the view when required. Single plants were cropped out of the images which contained more than one plant. Light intensity was measured using a standard lux meter. Under direct sun, it was more than 105 klux, while under shade it varied between 8 and 10 klux. Shutter time of the camera was kept between 3–6 ms (shade) and 0.2–0.3 ms (sunlight), respectively, to avoid under or over exposure (see Fig. 4).

2.1. Field setup and data acquisition

Data were collected in a field at the Department of Plant and Environmental Sciences, University of Copenhagen, Taastrup, Denmark. Sugar beet (*Beta Vulgaris* L.) were planted in late April 2013. Distance between crop rows and crop plants was 0.5 m and 0.15 m, respectively. The field was divided into two zones which were sown at two different dates, two weeks apart. Fertilizers were not used in the field.

A total of six image sets were acquired in June and July 2013. Two datasets with sugar beets in the 7th week of plantation at camera to ground distance of approximately 45 cm, one under direct sunlight and another under a shade, labeled $(7/45)_{sun}$ and $(7/45)_{shade}$ respectively. Two datasets with sugar beets in the 10th week, both under shade, at camera to ground distances of approximately 60 cm and 70 cm labeled $(10/60)_{shade}$ and $(10/70)_{shade}$, respectively. And finally, two datasets with the crop in the 12th week at camera to ground distance of 70 cm, one under sunlight and another under shade, labeled $(12/70)_{sun}$ and $(12/70)_{shade}$. Together the data in these six groups represented variations in terms of light, growth stage and scale (see Fig. 3 for sample images). Number of sugar beet and weed plants in each dataset were different subject to conditions of the fields (Table 1). The background contained mainly dry soil.

2.2. Image preprocessing and extraction of vegetation indices

Excess Green (ExG) (Woebbecke et al., 1995) was used to separate vegetation from soil, followed by Otsu thresholding (Otsu, 1979) to produce a complete binary image segmenting the vegetation against the background as shown in Fig. 5. A 5 × 5 median filter was then applied to remove any remaining noise producing a binary mask having white pixels for vegetation against black background. From the masked color images, vegetation indices given in Table 3 were extracted by averaging only the unmasked (vegeta-

tion) pixels, using normalized RGB values. A feature vector was thus created for each image in which every element corresponded to one of the indices.

2.3. Metrics for evaluation

In the task of weed detection, a weed plant detected as weed is a True Positive (TP) while a True Negative (TN) is a sugar beet plant detected as sugar beet. False Negatives (FN), on the other hand, are thistles misclassified as sugar beets. In certain industrial applications, such as weed or disease detection, along with the overall accuracy of the detection system, the FN is also an important factor. Any system with a higher accuracy but a substantial number of FNs may signify higher risk because if the weed or diseased plants are left out, they may quickly spread or multiply, compromising the net production even after the application of site specific treatment. In order to gage the performance in this regard, along with the accuracy, three other metrics are used:

$$Accuracy = \frac{TP + TN}{S} \tag{1}$$

$$Sensitivity = \frac{TP}{TP + FN} \tag{2}$$

$$Specificity = \frac{TN}{TN + FP} \tag{3}$$

$$FNR = \frac{FN}{TP + FN} \tag{4}$$

where S is the total number of samples in the test set, *FP* is the number of false positives (sugar beet detected as thistles) and *FNR* is the false negative rate. *Sensitivity* is the probability of a positive test given the plant in view is thistle (weed). On the other hand, *Specificity* is the probability of a negative test, given the plant is a sugar beet. Ideally, both should be higher, with sensitivity being slightly more important for weed or disease detection.

2.4. Methods

A matrix with rows corresponding to images and columns to indices was formed (from here on *vegetation indices* may be called *features*). Combining all the 14 features of the six groups produced a 474 × 14 matrix. Then each column was auto-scaled in MATLAB (R2013a), using function *zscore*, bringing each feature to a uniform scale with zero mean and unit variance. The data was split into test and training sets (50–50% from each species).

Principal Component Analysis (PCA) was used for analyzing the trends in the data. PCA reduces the number of variables/features which may be correlated, to fewer latent variables which are orthogonal and mutually uncorrelated. PLS toolbox (v7.5.2) for MATLAB from Eigenvector Research[3] was used for this purpose

---

[3] http://www.eigenvector.com/software/pls_toolbox.htm.

(a) ST 1 ms (b) ST 2.5 ms (c) ST 8 ms (d) ST 20 ms

Under Shadow (5-6 klux)

(e) ST 0.5 ms (f) ST 1 ms (g) ST 2.5 ms (h) ST 4 ms

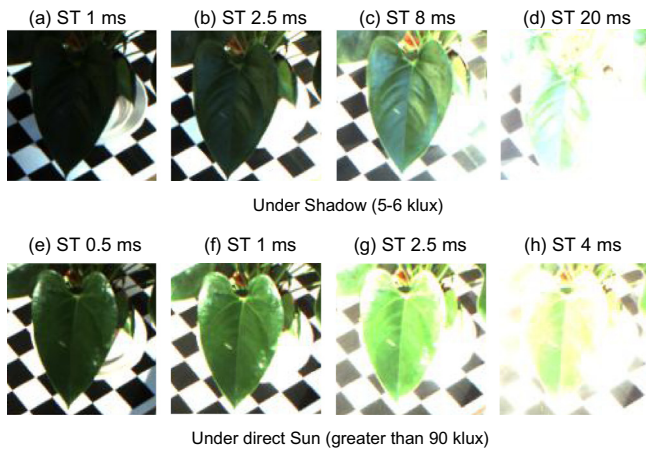Under direct Sun (greater than 90 klux)

Fig. 4. A leaf of Anthurium Andraeanum from another experiment (Kazmi et al., 2014) using the same camera. It shows the effect of exposure by controlling Shutter Time (ST: the duration of time for which the camera receives the incoming light) on the appearance of a leaf. In the current experiments the intensity of sunlight was slightly higher (being in summer) i.e. 8–10 klux under shade and greater than 105 klux under direct sun. Therefore, the selected shutter times (3–6 ms for shade and 0.2–0.3 ms for sun) avoided over or under exposure in each condition.

Table 1
Number of plants in each dataset.

Group No.	Label	Sugar beet	Thistle	Total
1.	$(7/45)_{sun}$	88	62	155
2.	$(7/45)_{shade}$	90	37	128
3.	$(10/60)_{shade}$	32	22	54
4.	$(10/70)_{shade}$	28	25	53
5.	$(12/70)_{shade}$	33	21	54
6.	$(12/70)_{sun}$	26	10	36
Total		297	177	474

and the effects of light, growth stage and scale on the separation of the two species were investigated.

To reduce the number of features through regression, *stepwise* function from MATLAB's Statistics Toolbox was used. A model was created by adding and removing features one by one given the enter and exit tolerances of 0.1 as proposed by Draper and Smith (1998).

In order to assess classification potential of the selected features, Linear Discriminant Analysis (LDA) and Mahalanobis

Distance (MD: with stratified covariance estimates) were applied using *classify* function from MATLAB's Statistics toolbox. For univariate classification, Standard Euclidean distance was used. To ensure sufficient cross validation, the results of 100 different random combinations of the training and test sets were averaged.

For histogram analysis, the frequencies of pixel intensities were normalized between [0 1] and divided into 256 bins [0 255] corresponding to 8 bit intensity data sampled from the ExG index. The ExG intensities were not auto-scaled in this case so that the relative variations in the raw index of the two species could be observed. The grouped sample standard deviation (σ_f) based on unbiased estimator was calculated using the MATLAB function shared by Trujillo-Ortiz and Hernandez-Walls (2012).

3. Results and discussion

Normalized features of group 1 are shown in Fig. 6. The box plot shows that the two plant species overlap in the normalized red, green, blue and gray channels, so much so that they cannot be easily discriminated. On the other hand, the computed vegetation indices are able to separate them. But there is a huge variance of light between sun (greater than 105 klux) and shade (8–10 klux) which can also be observed in the sample images in Fig. 3. Strong glare of the sun influences the perceived colors of the plants to a large extent (discussed in detail in Section 3.1). Therefore, if at the same scale and growth stage, the sun and shade data are combined, the variance within a given species increases, reducing the distinction (Fig. 7). Still some features, such as ExG, CIVE and GB are able to maintain an observable separation.

In order to get a more tangible measure of the classification potential of the calculated indices, we first assess them individually and then in combination. The results are shown in Fig. 8. The mean accuracy of certain features such as ExG and GB are very high, up to 93%. Other indices, such as CIVE, ERI, EBI and EGI also perform well. As expected, the raw color channels as well as the gray levels are not distinctive enough, with only normalized blue (Bn) performing slightly better.

As seen in Fig. 1, in the range of 400–500 nm, sugar beet absorb more blue light than thistles. The difference is maintained over, almost, the entire blue spectrum. This pattern reverses in the green channel and thistles absorb more light in between 500 and 600 nm. Once again a reversal takes place in the middle of the red spectrum between 600 and 700 nm.

The quantum efficiency curve of the sensor in Fig. 1 show that bandwidth of the filter is narrower for blue and red channels than

Table 2
Image resolutions and the corresponding Ground Sample Distances (GSD) at the selected ranges. Range implies camera to ground distance measured vertically. Leaf length is the approximate length along the central vein of a sugar beet leaf. A rectangular bounding box around a sample leaf in group 1 has approximately 3k pixels while in group 4 it has 80k pixels. Please note that the camera to leaf distance varied due to uneven local terrain and plant height.

Group nos.	Range (cm)	Resolution (pixels)	GSD (mm/pixel)	Leaf length (cm)
1 and 2	45	640 × 480	0.88	6–9
3	60	1280 × 960	0.59	12–18
4–6	70	1280 × 960	0.69	12–18

Input: Raw color image → ExG image → Otsu thresholding (Otsu,1979) + Median filtering (5x5) → Binary mask → ExG masked color image → Vegetation index vector extraction from unmasked pixels only
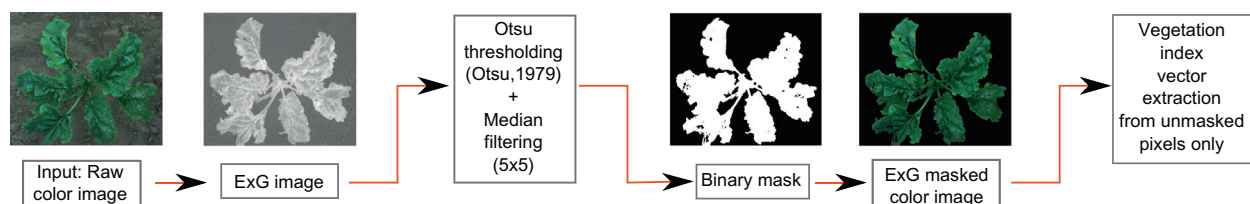
Fig. 5. Pre-Processing stages before vegetation index extraction.

Table 3
Color channels and vegetation indices used in this experiment.

Color index	Definition
Rn, Gn, Bn	R/(R + G + B), G/(R + G + B), B/(R + G + B)
Gray	0.2898 ∗ Rn + 0.5870 ∗ Gn + 0.1140 ∗ Bn
ExG (Woebbecke et al., 1995)	2 ∗ Gn − Rn − Bn
ExR (Meyer et al., 1998)	1.4 ∗ Rn − Gn
CIVE (Kataoka et al., 2003)	0.441 ∗ Rn − 0.811 ∗ Gn + 0.385 ∗ Bn + 18.78
ExGR (Meyer and Neto, 2008)	ExG − ExR
NDI (Woebbecke et al., 1992)	(Gn − Bn)/(Gn + Bn)
GB (Woebbecke et al., 1995)	Gn − Bn
RBI (Golzarian and Frick, 2011)	(Rn − Bn)/(Rn + Bn)
ERI (Golzarian and Frick, 2011)	(Rn − Gn) ∗ (Rn − Bn)
EGI (Golzarian and Frick, 2011)	(Gn − Rn) ∗ (Gn − Bn)
EBI (Golzarian and Frick, 2011)	(Bn − Gn) ∗ (Bn − Rn)

Fig. 7. Box plot of auto-scaled features for sugar beet and thistles of groups 1 and 2 (see Table 1) i.e. both sunlight and shade data together.
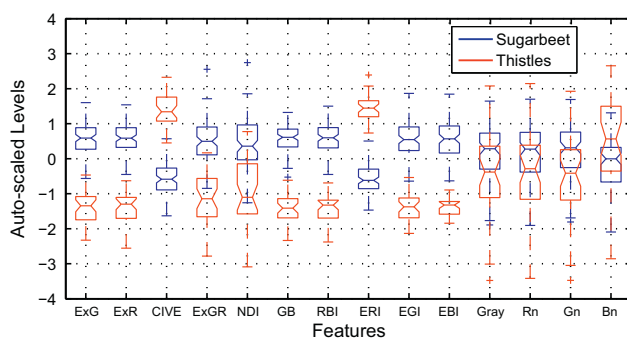

Fig. 6. Box plot of auto-scaled features for sugar beet and thistles of the group 2 (see Table 1) under shade.

the green one, which means that the camera can better capture the observable difference between the two species in these channels. But for the red spectrum, the difference between the species in the middle is not obvious. Besides, there is no prominent peak in sensor's response to wavelengths and hence the filter is almost equally averaging within the range of 600 to 700 nm. Therefore, in this case, normalized blue (Bn) is more distinctive than Gn and Rn.

In order to improve the overall accuracy and reduce FNR, usually more than one feature are combined. The following section elaborates our rationale for feature selection and combination.

3.1. Multivariate analysis

To analyze the trends in the data due to the variations in growth stage, illumination and scale, PCA was done. Fig. 9(a) shows the score plot of the first two principal components (PC1 and PC2) of the 14 features for all the groups. Together they explain the maximum variability of the data (about 85%). In the plot, two types of separation can be clearly observed; groups can be separated along PC1 and species along PC2. For a given growth stage and illumination, the subtle variations in scale do not seem to affect the distribution of the features. This can be observed through the similarity of the score plots in group 3 and 4 which are of the same age and acquired under shade but at 60 cm and 70 cm from the ground, respectively.

Growth stage, which is consistently varying for every pair, translates the data along PC1 which contributes towards almost 50% of the variability. Surprisingly, group 1 and 6 appear closer to each other. Even though being similar to group 2 and 5, respectively, in scale and age, they were obtained under direct sunlight. The effect of sunlight has reduced the influence of age, which is desired. But on the other hand, the features have also reduced
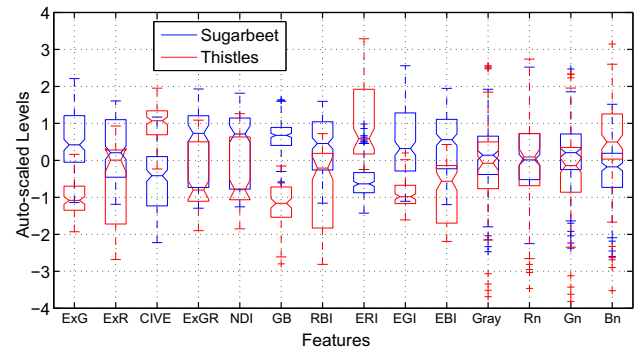
the separation along PC2 resulting in poor distinction in species. The change in illumination from shade to sun, therefore, affects the distribution of the data along both the principal components. By looking at their sister groups (2 and 5) we can observe that the species are better separated under shade conditions.

For a better classification, the influence of factors other than species on the variability of the data must be removed or at least reduced. For this purpose, we study the variable loadings in Fig. 9(b) alongside the score plot in Fig. 9(a). The loadings plot show that among the features encircled in red, EBI, RBI, ExR, Gray, Rn, Gn and Bn are largely contributing towards PC1 which according to the corresponding score plot is important in groups or growth stage separation. Meanwhile ExR and NDI are important for discrimination based on illumination as they appear to influence both PC1 and PC2 equally. We therefore, discard these features. This leaves behind GB, ExG, EGI, ERI and CIVE which primarily contribute towards PC2 and therefore are helpful for species discrimination. These are also the features offering the highest individual classification accuracy in Fig. 8. Since EGI and ExG are quite close, we keep only ExG. Therefore, the remaining features which are expected to explain the separation between the species by reducing the impact of growth stage and illumination are GB, ExG, CIVE and ERI.

Performing PCA again on these four features, we obtain the score plot and corresponding loadings in Fig. 10(a) and (b). In this score plot, PC1 accounts mainly for species while PC2 accounts for the illumination. This time, together the first two components explain 99% of the variability in the data. Again the cluster of groups 1 and 6 appears much farther from their sister groups (2 and 5). This means that although the effect of growth stage has been removed by carefully selecting features, the effect of sunlight vs shade could not be removed completely. Besides, it is also evident that a linear separation between the two species under shade is slightly different than in the sun.

Now that the data has been thoroughly analyzed, we combine more than one feature and compare their classification potential with individual indices.

3.2. Combination of indices

We know from Section 3 that the highest individual performance is given by ExG, GB and CIVE features (Fig. 8). The equations for calculating CIVE and ExG are numerically quite close but with an opposite sign (Table 3). Therefore, we initially tested the classification by only retaining ExG and GB indices.

The results are shown in Table 4. The overall accuracy was above 95% by both LDA and MD and with high specificity and sensitivity (between 94% and 97%). FNR was fairly low, between 3% and 4%. This shows that the most important features for thistle
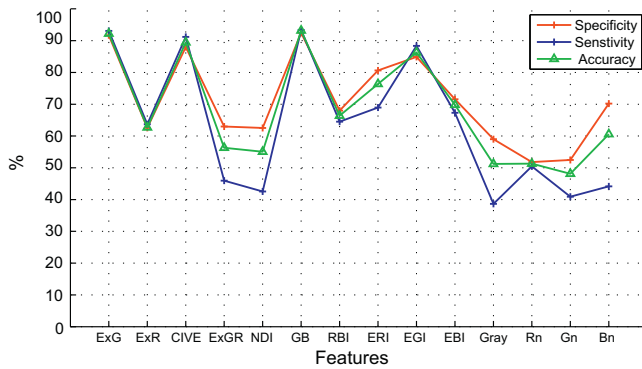
Fig. 8. Mean accuracy, sensitivity and specificity of individual indices using Euclidean distance.

and sugar beet classification are ExG and GB. These results were encouraging as they are slightly better than their individual performances.

We also identified four features through PCA in Section 3.1 which explained 99% of the variability in the data. Using those four

indices, we obtained an overall accuracy of 95% with specificity and sensitivity between 95% and 96% for MD and 91% and 98% for LDA. The number of false negatives, was also fairly low (between 1% and 5%). But as compared to the combination of ExG and GB only, it appears that inclusion of CIVE and ERI did not make much difference and only added processing overhead.

Another, most common method for feature selection is through regression. Stepwise linear regression was also used as explained in Section 2.4 on all the 14 features from the six groups. The model retained only nine features which are listed in Table 4. They acquired an accuracy above 97% with sensitivity and specificity between 96% and 99% and FNR between 2% and 4%. These are the highest net scores in the table.

It can be noted that both the LDA and MD based classification are comparable, as far as accuracy is concerned, making them both equally useful. High accuracy values are quite expected given the obvious separation between the species as already seen in Figs. 9 and 10. Still the FNR is slightly lower with MD.

It should be observed here that the features selected through regression may change by the addition or removal of a few samples or altering the enter/exit tolerances of the stepwise modeling process. Therefore, not all the features selected through regression
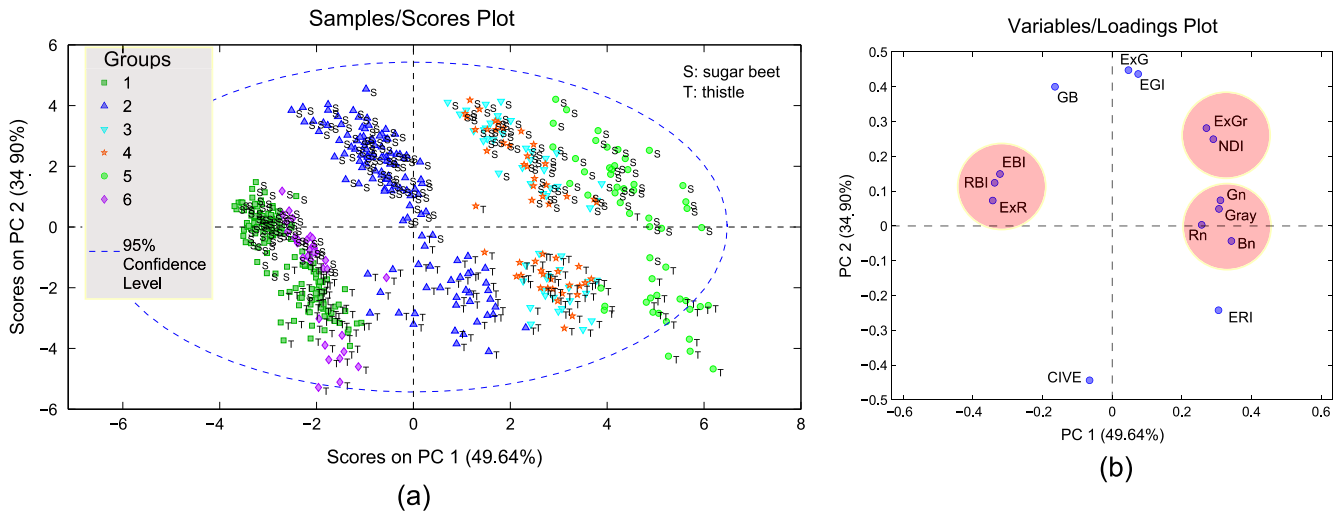

Fig. 9. (a) Score plot with the first two principal components for all the data from the six groups. (b) Corresponding loadings of the 14 features (Table 3).
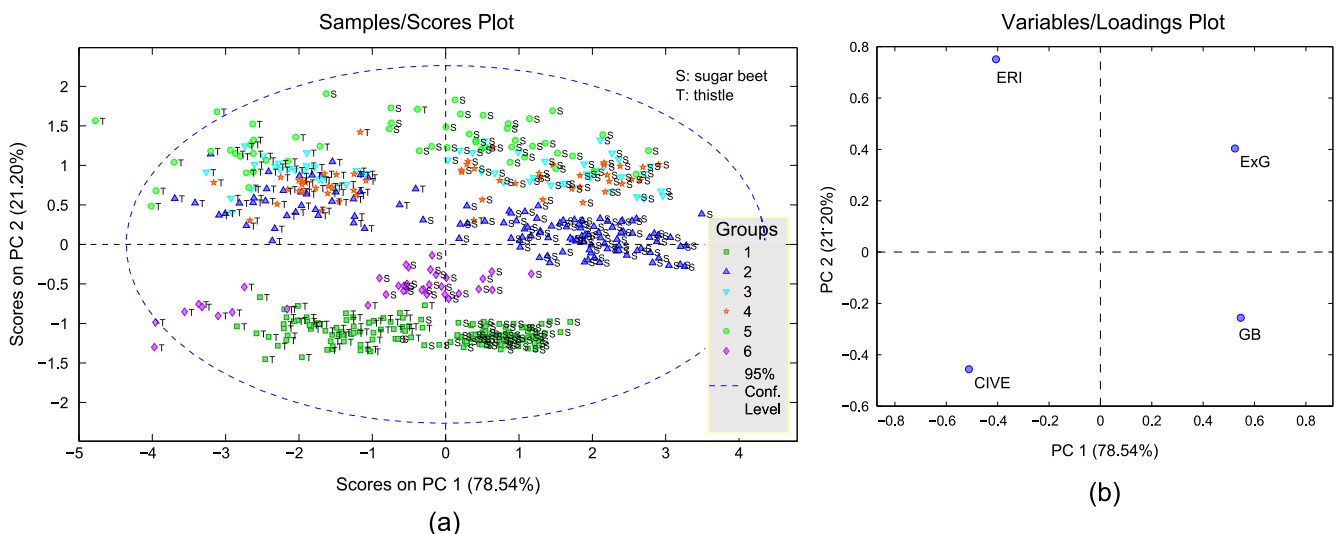

Fig. 10. (a) Score plot with the first two principal components for all the data from the six groups. (b) Corresponding loadings of the four selected features in Section 3.1, namely CIVE, GB, ERI and ExG.

Table 4
Classification results from the combination of features.

Classifier	Feature selection	Accuracy (%)	Sensitivity (%)	Specificity (%)	FNR (%)
LDA	Regression[a]	97.83	96.48	98.63	3.52
MD	–as above–	97.62	97.73	97.55	2.27
LDA	PCA[b]	95.77	95.46	95.96	4.54
MD	–as above–	94.05	98.53	91.38	1.47
LDA	Individual Performance[c]	95.33	96.34	94.73	3.66
MD	–as above–	95.48	96.44	94.90	3.56

[a] ExR, ExGR, NDI, GB, RBI, ERI, EGI, RN, GN.
[b] ExG, CIVE, GB, ERI.
[c] ExG, GB.

may be intuitive as the model is customized to the given set only. This is implied in the nine selected features which include ExGR, NDI, RBI, Rn, even though in the PC analysis in Section 3.1, we have seen that these features appear to contribute more towards growth stage separation than species distinction.

3.3. Validation tests

Now that we have established the fact that a combination of only a few of the features has enough potential to segregate thistles and sugar beet with sufficient accuracy, we trained our system on a model created by using the three different feature combinations listed in Table 4 for the entire unnormalized data (i.e. 474 samples) and annotated the pixels in images containing both thistles and sugar beet. These images were not used in the training. The results are shown in Fig. 11 for a visual analysis. In these images, pixels classified as thistles and sugar beet are marked red and blue, respectively.

Fig. 11 (1) and (2) were acquired under sun and shade, both in the 7th week after plantation (similar to groups 1 and 2). On comparison of the annotations, we can observe that the regions of sugar beet and thistles are marked clearly in the image under shade but ambiguously for the image under sunlight. In the score

plot of Fig. 9, we have already seen that under the sunlight, the perceived color separation between two species was reduced. The ambiguity in annotation is the consequence of this closeness.

Fig. 11 (3) and (5) were both acquired under shade, in the 10th and 12th week, respectively (similar to group 3 and 5). Although the regions pertaining to sugar beet and thistles can be identified, still some pixels, specially on the flanks of the sugar beet leaf are detected as thistles. This is due to the fact that the bigger plants with their complicated canopies produce varying shades in the perceived colors. We discuss this aspect in more detail in the following section by interpreting the histograms.

3.4. Histogram analysis

The histograms of only ExG index of single plants of the subject species are shown in Fig. 12 for all the groups. Even though from the same species and groups, each plant is different from another. The combination of every thistle and sugar beet plant in a given group is not feasible. So, we randomly selected one plant from each species to get the histograms shown in the figure. The reason for only choosing ExG is that this is one of the features with highest individual performance and other indices with similar performances, such as GB and CIVE are expected to allow a similar analysis.
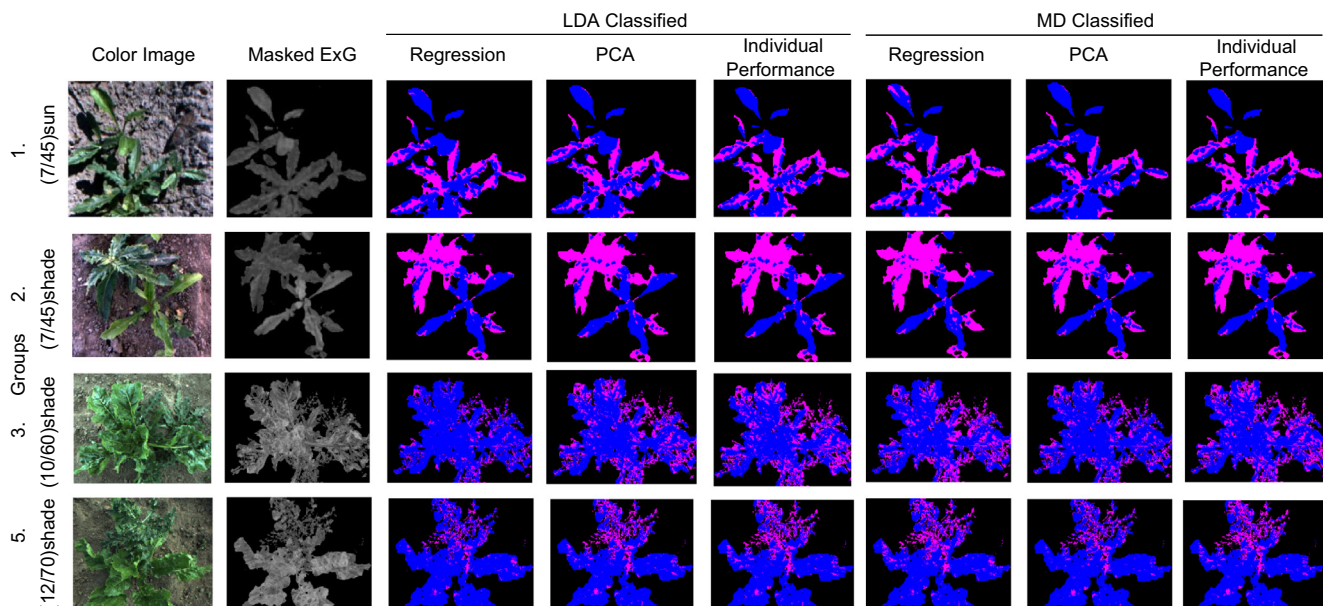

Fig. 11. Images annotated by classifiers trained on the unnormalized data. Sugar beet pixels appear blue and thistle pixels appear red. Features were selected based on individual performance, PCA and regression analysis (Table 4). (For interpretation of the references to color in this figure legend, the reader is referred to the web version of this article.)
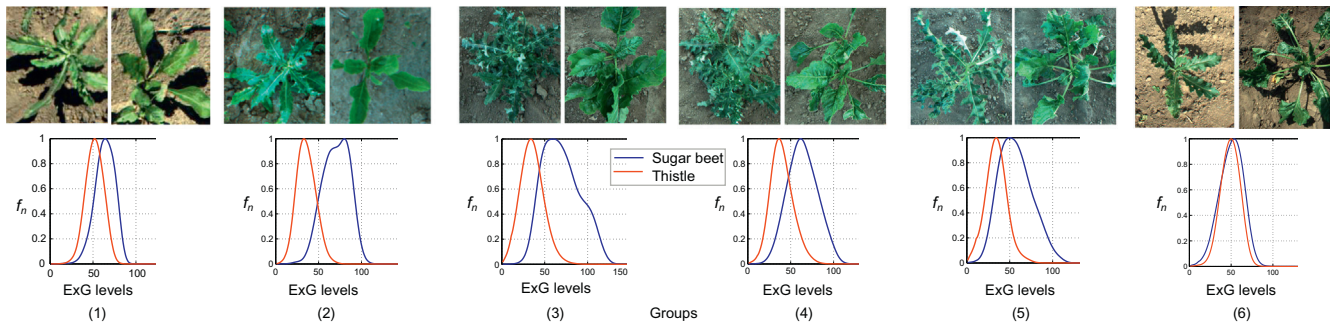
Fig. 12. Sample histograms of the subject species in the six groups (Table 1). f_n is the normalized number of pixels with the ExG levels in the range [0255].

For classification, our classifiers were trained on the mean values of indices and the mean intensity levels follow the peaks of their corresponding histograms. Except for a few odd samples, the peaks of the species in all the groups are separable and thus a high classification accuracy is a natural outcome. But for the perfect annotation of all the pixels in the validation set, the two histograms should ideally be well apart, leaving behind no overlap. Unfortunately, from the histograms in Fig. 12, it is evident that this is not the case. Due to the overlapping of the histograms of the two species, certain pixels of sugar beet plants can be marked as thistles or vice versa. This is the result of the nature of the appearance of the plants, which are both green after all. The only thing we can do is to minimize the overlap.

The extent of the overlap of histograms depends on the separation between the peaks as well as the spread of the histogram. The narrower the histograms and the farther the peaks, the lesser is the overlap. To measure the width of the histograms and separation of the peaks, we use twice the standard deviation ($2\sigma_f$) and the peak difference, both specified in the number of bins (total 256 bins from 8 bit data). Although, as we said, each plant is different from another no matter it is from the same specie and group, we average the histograms in order to get a net impression. The results are reported in Table 5. From these results, we can conclude that the factors affecting the histograms' width and peak separation are the following:

3.4.1. Illumination

Under shade, the histogram peaks are well separated as compared to the data acquired under sunlight. For example, for group 2 and 1, the peak difference reduces from 22 to 17 due to sunlight. On the other hand, under sunlight, the histogram is narrower than under the shade. It appears that the fine shifts between the color intensity levels are more noticeable when the strong glare of the sun is blocked, thus producing wider histograms. Again, this difference from sun to shade data is more significant in younger plants than older ones as can be observed in the data in Table 5 groups 1, 2 and 5, 6, respectively.

3.4.2. Plant size

In the fields, the plants tangible by size or age are mainly the crop (sugar beet) which are planted at a specific date. At an earlier growth stage, due to smaller size, the crop canopy is less complicated as can be seen in Fig. 13(b). This prevents the leaves from bending and folding either due to wind, water stress or weight. These factors get dominant as the plant grows (Fig. 13(a)) and the leaf area increases. Due to strong winds leaves can flip exposing the under side which may have very different colors, thus changing the histograms. Fig. 13(b) shows local curvatures appearing on the sugar beet leaves as it grows, which introduces greater variability in the local surface normals among different segments on the leaf surface, due to which the color perception is affected.

Table 5

Average values from the histograms of ExG index in the range [0255]. Peak Difference (PD_{av}) is the average number of bins between the peaks of the histograms of thistle and sugar beet plants of a group. $2\sigma_{f(av)}$ is the average standard deviation of the sugar beet histograms of a group.

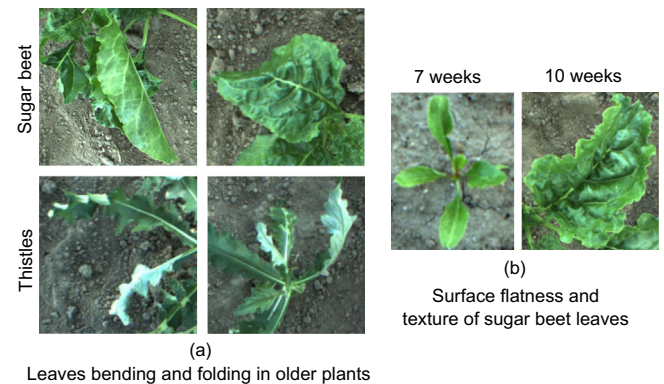| Group nos.	Label	PD_{av}	$2\sigma_{f(av)}$
1	$(7/45)_{sun}$	17	33.40
2	$(7/45)_{shade}$	22	41.97
3	$(10/60)_{shade}$	23	49.63
4	$(10/70)_{shade}$	20	45.90
5	$(12/70)_{shade}$	20	47.76
6	$(12/70)_{sun}$	19	41.56

Fig. 13. Leaf shape complications in older plants. (a) Plant samples from groups 3 and 5 (later growth stages). Leaf bending and folding can be observed, which introduces changes in the shades of the perceived colors. (b) Leaf surface comparison for young (group 2) and older (group 3) sugar beet leaves. Younger plants have much smoother texture and planar surface. (For interpretation of the references to color in this figure legend, the reader is referred to the web version of this article.)

Hence the number of pixels with color levels far away from the mean increase, producing wider histograms which increases the overlap. Comparatively, the younger plant leaves are flatter.

3.4.3. Image scale

Slight changes in the distance between the camera and the plant does not seem to affect the spread of the histogram a lot but it slightly alters the peak separation (Table 5, group 3 and 4). It appears from these groups that the closer the camera, the higher the peak separation. Perhaps, the increased distance between the camera and the plant reduces the fine sampling of color levels, thus reducing the peak separation.

Other than these prominent factors, exposure time of the camera as well as the light intensity, especially under shade (which can vary over a wide range) also affects the perceived color levels.

3.5. Discussion

It can be observed in Fig. 1 that the difference in the spectral response of sugar beet and thistle in blue and green channels is augmented by the factor, green minus blue. Therefore, the indices using this factor (e.g. GB, ExG, CIVE and EGI) offer comparatively higher individual classification potential.

Woebbecke et al. (1995) found that shifting from direct sun to shade influenced each of the three color channels almost equally, yet in their experiments, one can observe that some channels could be slightly more influenced than the others. El-Faki et al. (2000a) also found out that the effect of variation in illumination on perceived colors was significant but relative. In their experiments they showed that the R, G and B plates slightly reduced their separation when illumination was increased. We have also observed the same. In Fig. 9, the sunlight translates the data along the principal components, overwhelming the influence of growth stage and scale and reducing the separation between the species. The histogram analysis revealed that the plant imaging under direct sunlight, although, narrows the histogram, but it is still not suited due to slightly reduced peak difference between thistle and sugar beet plants as the histograms are drawn closer. This can be observed in Fig. 12 (1) and (2). Under the sun, in worst cases, the histograms can even be almost merged (Fig. 12 (6)) due to which the annotation under sun (Fig. 11 (1)) is not optimal. Whereas, under a shade, the separation is increased. This is the reason that El-Faki et al. (2000b) recommended imaging under dimmer illumination. Therefore, we also conclude that imaging under a shade should be preferred.

As far as exposure control is concerned, since the normalized color values were used to compute indices (i.e. Rn, Gn and Bn), the effects of subtle variations in exposure or illumination were minimal (Woebbecke et al., 1995; Golzarian and Frick, 2011). This is mainly important for imaging under a shade since the distance between the plant and the shade itself affects the shadow and its darkness due to which the illumination under a shade varies.

El-Faki et al. (2000b) argued that their plants at latter growth stages were classified better. This was due to the fact that the weed stems turned red (pigweed) as they grew. The species in our case have no such feature. This is a major limitation in color based vegetation analysis. If the perceived colors of the target species are close, results may not be encouraging. Bigger thistle and sugar beet plants due to their larger leaf surface and significant surface texture (Fig. 11 (3) and (5)) make variations due to wind and illumination more influential even under shade. Hence, the best compromise between width of the histogram, the peak separation and the environmental factors can be reached by adopting the situation in group 2 shown in Fig. 11 (2) and Table 5 (2) i.e. younger plants under shade.

To increase the robustness of the system and to include more species of weed, shape features are helpful. But in order to include shape features, at least a single plant or sometimes, an organ such as a leaf, must be identified in the image, without occlusions (El-Faki et al., 2000b; Sogaard, 2005; Golzarian and Frick, 2011). Shape features vary with growth stage. Where environmental factors such as sunlight and water stress can affect the perceived color of the plants, wind and occlusion affects the shape perception. Sunlight can be blocked or diffused by introducing a shade, but it is difficult to avoid wind and occlusion.

Therefore, for any group of species with some sustained separation in more than one color index, it is convenient to avoid shape features. This can reduce the complexity of the system by sparing the computationally expensive task of resolution of plant overlap and leaf segmentation which may require 3D imaging (Dellen et al., 2011; Alenya et al., 2011) and 3D sensing has its own set of challenges, especially when it comes to outdoor scenarios (Kazmi et al., 2014).

Since the classification framework proposed in this article is merely using color information, the processing efficiency is very high making it suitable for real-time systems without the reliance on specialized hardware. In field application, for example, this weed detection system can be coupled with cameras and controllers of spray nozzles on a tractor mounted sprayer boom (Lund et al., 2011). Human driven tractor demands very fast data processing, in which case, working with only two indices (ExG and GB) will only slightly compromise the classification performance while allowing higher throughput.

4. Conclusions

In this article, we have presented a practical and efficient solution to the problem of weed detection in sugar beet fields. Using only vegetation indices, we have shown that thistles can be detected with a very high accuracy, up to 97% in the field images. The validation tests showed that we can also detect highly occluded weed plants thus avoiding 3D sensing.

Color based classification is highly dependent on the quality of the color perception which demands use of cameras with fine tuned and calibrated color filters. Environmental factors, such as sunlight, still pose the biggest challenge though. Therefore, a robust mechanism for blocking sunlight must be used.

We have also argued that the increase in the size of the plants due to age, makes the effect of light and wind more influential. Therefore, for an optimal performance, the task of weed detection must be carried out at an earlier growth stage. This is also in line with the agronomic principles as the sooner the weeds are removed, the lesser is the production loss.

For increasing the robustness against environmental factors of a field deployable system, classifiers must be trained or calibrated in the subject field and setting and with the chosen imaging setup.

Addition of shape feature may widen the scope by making it possible to include more species, but the challenge of occlusion remains. In future, avoiding the computationally expensive task of leaf segmentation, we intend to exploit the shapes of the leaves' edge fragments in combination with color indices for weed detection.

Acknowledgment

References

Åstrand, B., Baerveldt, A., 2002. An agricultural mobile robot with vision-based perception for mechanical weed control. Auton. Robots 13 (1), 21–35, http://link.springer.com/article/10.1023/A:1015674004201.

Alenya, G., Dellen, B., Torras, C., 2011. 3D modelling of leaves from color and ToF data for robotized plant measuring. In: IEEE International Conference on Robotics and Automation. Shanghai, China, pp. 3408–3414 <http://www.iri.upc.edu/research/webprojects/pau/_IMATGES/figspapers/Alenya_icra11.pdf>.

Andreasen, C., Stryhn, H., 2012. Increasing weed flora in Danish beet, pea and winter barley fields. Crop Protect. 36, 11–17, <http://linkinghub.elsevier.com/retrieve/pii/S0261219412000142>.

Backes, M., Jacobi, J., 2006. Classification of weed patches in QuickBird images: verification by ground truth data. EARSeL eProc. 5 (2), 173–179, <http://eproceedings.org/static/vol05_2/05_2_backes1.pdf>.

Christensen, S., Heisel, T., 2003. A decision algorithm for patch spraying. Weed Res. 43, 276–284, <http://onlinelibrary.wiley.com/doi/10.1046/j.1365-3180.2003.00344.x/full>.

Christensen, S., Søgaard, H.T., Kudsk, P., Nørremark, M., Lund, I., Nadimi, E.S., Jørgensen, R., 2009. Site-specific weed control technologies. Weed Res. 49 (3), 233–241, <http://blackwell-synergy.com/doi/abs/10.1111/j.1365-3180.2009.00696.x>.

Dellen, B., Alenya, G., Foix, S., Torras, C., 2011. Segmenting color images into surface patches by exploiting sparse depth data. In: Workshop on Applications of Computer Vision (WACV). IEEE, Kona, Hawai, pp. 591–598, <http://ieeexplore.ieee.org/xpls/abs_all.jsp?arnumber=5711558>.

Draper, N.R., Smith, H., 1998. Selecting the best regression equation. In: Applied Regression Analysis, third ed. Wiley & Sons, pp. 342–343 (Ch. 15).

Ehsani, M., Upadhyaya, S., Mattson, M., 2004. Seed location mapping using RTK GPS. Trans. Am. Soc. Agricult. Biol. Eng. ASABE 47 (3), 909–914, <http://asae.frymulti.com/abstract.asp?aid=16088&t=1>.

El-Faki, M., Zhang, N., Peterson, D., 2000a. Factors affecting color-based weed detection. Trans. ASAE 43 (4), 1001–1009, <http://www.researchgate.net/publication/235897747_FACTORS_AFFECTING_COLOR-BASED_WEED_DETECTION/file/32bfe513ee0c4864f0.pdf>.

El-Faki, M., Zhang, N., Peterson, D., 2000b. Weed detection using color machine vision. Trans. ASAE 43 (6), 1969–1978, <http://www.researchgate.net/publication/235897833_WEED_DETECTION_USING_COLOR_MACHINE_VISION/file/32bfe513ee4fed93bc.pdf>.

FAOSTAT, 2011. Food and Agricultural Organization of the United Nations <http://faostat3.fao.org/> (retrieved 26.02.14).

Feyaerts, F., Pollet, P., Van Gool, L., Wambacq, P.C., E1 - Rust, R.H., E1 - Larson, W.E., P.E.R., 1999. Sensor for Weed Detection Based on Spectral Measurements, pp. 1537–1548 <https://dl.sciencesocieties.org/publications/books/abstracts/acsesspublicati/precisionagric4b/1537>.

Golzarian, M.R., Frick, R.a., 2011. Classification of images of wheat, ryegrass and brome grass species at early growth stages using principal component analysis. Plant Meth. 7 (1), 28, <http://www.pubmedcentral.nih.gov/articlerender.fcgi?artid=3195210&tool=pmcentrez&rendertype=abstract>.

Golzarian, M., Lee, M., Desbiolles, J., 2012. Evaluation of color indices for improved segmentation of plant images. Trans. ASABE 55 (1998), 261–273, <http://cat.inist.fr/?aModele=afficheN&cpsidt=25698693>.

Jafari, A., Mohtasebi, S., Jahromi, H., Omid, M., 2006. Weed detection in sugar beet fields using machine vision. Int. J. Agricult. Biol. 8 (5), 602–605, <http://www.fspublishers.org/ijab/past-issues/IJABVOL_8_NO_5/8.pdf>.

Kataoka, T., Kaneko, T., Okamoto, H., Hata, S., 2003. Crop growth estimation system using machine vision. In: Proceedings of IEEE/ASME International Conference on Advanced Intelligent Mechatronics (AIM), vol. 2, pp. 1079–1083 <http://ieeexplore.ieee.org/lpdocs/epic03/wrapper.htm?arnumber=1225492>.

Kazmi, W., Bisgaard, M., Garcia-Ruiz, F., Hansen, K., la Cour-Harbo, A., 2011. Adaptive surveying and early treatment of crops with a team of autonomous vehicles. In: European Conference on Mobile Robots. Orebro, Sweden, pp. 253–258 <http://aass.oru.se/Agora/ECMR2011/proceedings/papers/ECMR2011_0036.pdf>.

Kazmi, W., Foix, S., Alenyà, G., Andersen, H.J., 2014. Indoor and outdoor depth imaging of leaves with time-of-flight and stereo vision sensors: Analysis and comparison. ISPRS J. Photogram. Rem. Sens. 88, 128–146, <http://www.sciencedirect.com/science/article/pii/S0924271613002748>.

Lopez-Granadoz, F., 2011. Weed detection for site-specific weed management: mapping and real-time approaches. Weed Res. 51 (1), 1–11, <http://dx.doi.org/10.1111/j.1365-3180.2010.00829.x>.

Lund, I., Jensen, P.K., Jacobsen, N.J., Rydahl, J.T., 2011. The intelligent sprayer boom – a new generation of sprayers. Aspects Appl. Biol. 99, 439–442.

Mathiassen, S.K., Bak, T., Christensen, S., Kudsk, P., 2006. The effect of laser treatment as a weed control method. Biosyst. Eng. 95 (4), 497–505, <http://linkinghub.elsevier.com/retrieve/pii/S1537511006002984>.

Meyer, G.E., Neto, J.A.C., 2008. Verification of color vegetation indices for automated crop imaging applications. Comp. Electron. Agricult. 63 (2), 282–293, <http://linkinghub.elsevier.com/retrieve/pii/S0168169908001063>.

Meyer, G.E., Mehta, T., Kocher, M.F., Mortensen, D.A., Samal, A., 1998. Textural imaging and discriminant analysis for distinguishing weeds for spot spraying. Trans. ASAE 41 (4), 1189–1197, <http://cat.inist.fr/?aModele=afficheN&cpsidt=1598792>.

Miller, S., Fornstrom, K., Mesbah, A., 1994. Canada thistle control and competition in sugarbeets. J. Sugar Beet Res. 31 (3-4), 87–96, <http://cat.inist.fr/?aModele=afficheN&cpsidt=3469828>.

Monaco, T.J., Grayson, A.S., Sanders, D.C., 1981. Influence of four weed species on the growth, yield, and quality of direct-seeded tomatoes (Lycopersicon esculentum). Weed Sci. 29 (4), 394–397, <http://www.jstor.org/stable/4043319>.

Nieuwenhuizen, A.T., Tang, L., Hofstee, J.W., Müller, J., Henten, E.J., 2007. Colour based detection of volunteer potatoes as weeds in sugar beet fields using machine vision. Prec. Agricult. 8 (6), 267–278, <http://link.springer.com/10.1007/s11119-007-9044-y>.

Otsu, N., 1979. A threshold selection method from gray-level histograms. IEEE Trans. Syst., Man Cybernet. 9 (1), 62–66.

Pérez, A., López, F., Benlloch, J., Christensen, S., 2000. Colour and shape analysis techniques for weed detection in cereal fields. Comp. Electron. Agricult. 25, 197–212, <http://www.sciencedirect.com/science/article/pii/S016816999900068X>.

Point Grey, R., 2013. Chameleon Imaging Performance (rev1.1), 4.

RHEA, 2011. Robot Fleets for Highly Effective Agriculture and Forestry Management <http://www.rhea-project.eu/> (retrieved 12.03.14).

Sogaard, H., 2005. Weed classification by active shape models. Biosyst. Eng. 91 (3), 271–281, <http://linkinghub.elsevier.com/retrieve/pii/S1537511005000772>.

Tosaka, N., Hata, S.-i., Okamoto, H., Takai, M., 1998. Automatic thinning mechanism of sugar beets (Part 2). J. Japan. Soc. Agricult. Mach. 60 (2), 75–82.

Trujillo-Ortiz, A., Hernandez-Walls, R., 2012. gstd: Standard deviation of a grouped sample <http://www.mathworks.com/matlabcentral/fileexchange/38318-gstd> (retrieved 04.09.14).

Tyr, S., Veres, T., 2012. Top 10 of the most dangerous weed species in sugar beet stands in the Slovak republic. Res. J. Agricult. Sci. 44 (2), 100–103, <http://search.ebscohost.com/login.aspx?direct=true&db=aph&AN=90267152&site=ehost-live>.

Vrindts, E., De Baerdemaeker, J., Ramon, H., 2002. Weed detection using canopy reflection. Prec. Agricult. 3 (1), 63–80, http://dx.doi.org/10.1023/A:1013326304427.

Woebbecke, D.M., Meyer, G.E., Von Bargen, K., Mortensen, D.A., 1992. Plant species identification, size, and enumeration using machine vision techniques on near-binary images. Optics in Agriculture and Forestry, vol. 1836. SPIE, pp. 208–219, http://dx.doi.org/10.1117/12.144030.

Woebbecke, D., Meyer, G.E., Von Bargen, K., Mortensen, D.A., 1995. Color indices for weed identification under various soil, residue, and lighting conditions. Trans. ASAE 38 (1), 259–269, <http://cat.inist.fr/?aModele=afficheN&cpsidt=3503524>.